

Molecular Modeling and Chemical Synthesis of New Safrol Oxime Ether Derivatives

Mariana G. R. Silva,¹*,^{a,b} Marcia P. Veloso,^{a,b} Thaynan A. B. Chagas,^a
Mirian M. Cordeiro,^a Levy B. Alves,^b Paloma A. G. Monti^a and Ruth V. Souza^a

^aLaboratório de Pesquisa em Química Farmacêutica (LQFar),
Faculdade de Ciências Farmacêuticas, Universidade Federal de Alfenas,
Rua Gabriel Monteiro da Silva, 700, 37130-000 Alfenas-MG, Brazil

^bLaboratório de Modelagem Molecular e Simulação Computacional (MolMod-CS),
Faculdade de Biotecnologia, Universidade Federal de Alfenas,
Rua Gabriel Monteiro da Silva, 700, 37130-000 Alfenas-MG, Brazil

Leishmaniasis, a neglected tropical disease with a high worldwide incidence, is considered a public health issue in Minas Gerais and Brazil, with a high degree of morbidity, not to mention the lack of therapeutic arsenal. The cysteine protease (rCPB2.8) and cyclin dependent kinase (CRK3), important enzymes for the parasite's feasibility, were the targets chosen for investigation of the new drugs. The following study aimed to analyze several oximic derivatives starting from safrol, which can present an affinity profile for selected molecular targets using tools from molecular modeling and bioinformatics, planning and synthesis of brand new substances being tested for leishmanicidal drugs. The study allowed to verify that three oximic derivatives (**5a**, **5f** and **5h**) presented high affinity for the CRK3 enzyme, and that the compounds **5c** and **5g** presented good interaction by the amino acids of the catalytic site of the rCPB2.8 enzyme with atomic distances capable of generating covalent bonds, which are essential for enzyme inhibitory activity.

Keywords: leishmaniasis, molecular modeling, safrol oxime ether, CRK3, rCPB2.8

Introduction

Leishmaniasis is a disease affecting more than 12 million people worldwide, with more 350 million at risk of infection by the parasite of the genus and almost 2 million new cases reported annually.¹ It is a parasitic disease caused by protozoa of the genus *Leishmania* and transmitted through a sting by the female of the insect of the genus *Lutzomyia* and *Phlebotomus*, being able to present itself in three main forms, visceral, cutaneous and mucocutaneous.² As a neglected disease, it affects poorer populations and is directly related to poor nutrition, precarious housing, weakened immune system and lack of financial resources.³ In 2018, the Health Surveillance Department (SVS) presented a survey regarding the scenarios of visceral leishmaniasis in Brazil, in which it reported the number of new cases *per* state in the country. It was thereby reported that the state of Minas Gerais is the second state in which cases of the disease increased the most in 2016.⁴

Furthermore, during the years 2000 and 2011, only 4% of approved drugs, including 1% new ones, referred to the treatment of neglected diseases, largely due to the cut in funding by industry and several other agencies in the development of such products.⁵ The disease still has a problematic treatment, with a limited and barely accessible therapeutic arsenal available, in the case of expensive and toxic drugs.⁶

Some new potential molecular targets for the development of antiparasitic drugs are described in the literature. In this regard, the identification of key differences between host and parasite metabolism is of great importance for the development of new compounds with the desired pharmacological activity.⁷ A study⁸ pointed out that the cysteine protease (rCPB2.8) enzyme is essential for the virulence and survival of the *Leishmania* parasite and understanding the mechanism of its inhibition and chemical entities interacting with the enzyme's active site makes of it a potential target to be explored.⁸ Its function is related to protein metabolism. The catalytic residues of this class of enzymes are cysteine, histidine and asparagine

*e-mail: marigrisola@gmail.com

amino acids. Peptide substrates hydrolyzed by this class of enzyme are known to be highly basic and some possibly hydrophobic.⁹⁻¹¹ These enzymes have an important role in *Leishmania*, such as virulence, maintenance of viability and morphology of the parasite, invasion of the host's mononuclear phagocytic system and the modulation of its immune response, thus constituting attractive chemotherapy targets in the treatment of leishmaniasis.¹²

Likely, cyclin dependent kinase (CRK3) activity inhibitors prove to be possible targets for the development of new leishmanicidal drugs, among protein kinase inhibitors adenosine triphosphate (ATP)-competitor inhibitors stand out.^{13,14} It is known that the structure *vs.* activity of the CRK3 enzyme is closely linked to the active site binding ATP. CRK3 is a cyclin-dependent serine/threonine kinase protein of the CDK (cyclin dependent kinase) family isolated in *Leishmania*, essential for the transition through the G2 phase (phase in which the cell prepares for mitosis) to M (mitotic), regulating the cell cycle of the parasite; its inhibition leads to cell death due to apoptosis.¹⁴⁻¹⁶ The identification of ATP-competitor inhibitors is a promising field in the study of new drugs, since ATP is the legitimate cofactor of a CDK.¹⁵ Small changes in amino acid sequences at ATP binding sites of *Leishmania* CRK3 with respect to human CDK2, evidenced in a study,¹⁶ can be used as targets for selective inhibition of CRK3. The main divergence in CRK3 amino acid side chains with human CDK2 is the replacement of PHE82 (phenylalanine) and LEU83 (leucine) with tyrosine and valine in CRK3, GLN85 (glutamine) is replaced by alanine and HIS84 (histidine) by glutamate.¹⁶

The use of safrol (4-allyl-1,2-methylenedioxybenzene), natural allybenzene considered as a starting product for the new proposed series of oximic ethers, has a broad distribution in the vegetable kingdom, carrying an important phenolic ether found in essential oils extracted from plants such as sassafras (*Ocotea* sp.), of sassafras cinnamon (*Ocotea pretiosa* Mez) and long pepper (*Piper hispidinervum*).¹⁷

Choosing natural products as an alternative for the development of new drugs shows a good study proposal from the beginning, due to the fact that they have several benefits and biological activities when isolated.¹⁸ Linked to this idea, it is known that oximes (general formula: $RR'C=NOH$) and their derivatives (such as oximic ethers and esters) also have protozoic, antifungal and anticancer actions.¹⁹⁻²¹ It is known that amphotericin B, an antifungal currently used in the treatment of leishmaniasis, has activity against the parasite, therefore there are some studies of oxime ethers acting with high antifungal potential, such as that reported by Xie *et al.*²² and the discovery of

oxiconazole, most popularly known and reported antifungal oximic ether.²³

The following study aims to establish a relationship between the planned chemical structure and the potential targets of *Leishmania* selected, through molecular modeling approaches and the choice of a rationally planned structure for the study. Choosing the structure is directly related to substrates already reported in the literature, such as arginase and metacaspases, as potential inhibitors of selected enzymes.

The structure *vs.* activity relationship established by Mott *et al.*,²⁴ when studying the structure of CPB inhibitors, associated the presence of electronegative atoms linked to an aromatic ring with better activity, in addition of showing that a hydrophilic portion was well tolerated, plus the affinity for basic portions, which is the case with the proposed oximic nitrogen and the possibility of generating hydrogen interactions with cysteine from the active site in that portion; there is also the presence of the aromatic ring replaced with more and less electronegative atoms and more hydrophilic groups for comparison purposes, not to mention the twin methyl making this portion of the molecule more hydrophobic.

Very similar are the CRK3 enzyme inhibitors, planned as of the proposed similarity of functional groups of known drugs interacting with this class of enzymes, such as gefitinib, an ATP-competitive inhibitor of a protein tyrosine kinase, which has a methoxide group, a basic morpholine group and the presence of halogens (chlorine and fluorine) similar to the molecules proposed herein, thus seeking to inhibit the cyclin 3-dependent kinase enzyme present in species of *Leishmania*.²⁵

All the final compounds proposed (**5a-5h**) are new and not reported yet. The choice of parts of molecule was based on inhibitors known in the literature,^{24,25} CRK3 and CPB enzyme inhibitors mostly have in common a two-ring system interspersed by a spacer element, usually represented by a secondary amine (Figure 1), to resemble this characteristic of the molecule, oxime was chosen, besides to the presence of existing halogens in inhibitors of CDK2 (CRK3 analogue) and also associated with potential anticancer agents.²¹ The exclusion of asymmetric center of α -carbon to oximic carbon was also important, making the structure simpler stereochemically. One of the objectives of the work was the determination of a simple and reproducible synthetic route, as the oxime ether becomes attractive because it depends on only two steps to carry it out from a carbonyl.²⁶

Few studies have listed oximes and safrol as leishmanicidal agents, making this an important approach in the scientific field.

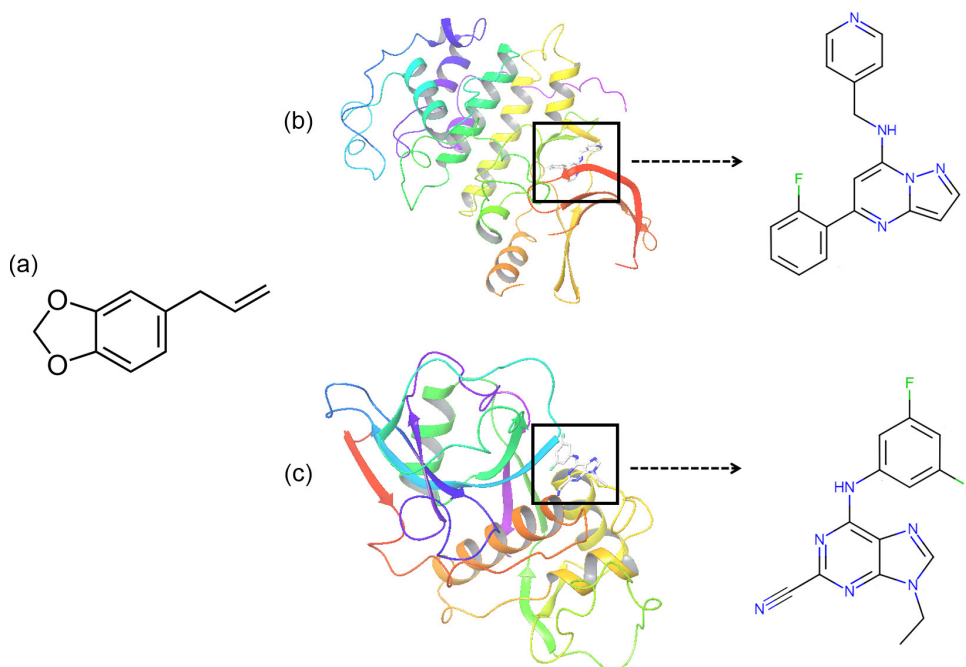


Figure 1. (a) Molecular structure of safrol. (b) Crystal structure of cyclin-dependent kinase CDK (PDB: 2R3I) with inhibitor and CRK3 analogue. (c) Crystal structure of cruzain's cysteine protease (PDB: 3I06) with inhibitor and CPB analogue.

Experimental

Homology modeling

The MODELLER²⁷ software version 9.16 was used to carry out the molecular modeling by homology, with the aid of the PROCHECK²⁸ program, in addition to other online software for its validation.^{29,30}

CRK3

The construction of the three-dimensional model by structural homology for the CRK3 protein was based on the study described in the literature by Pereira *et al.*,¹⁵ as of the structure already fixed in the Protein Data Banking³¹ database (PDB 2R3I, 1.28 Å).

rCPB2.8

The construction of a three-dimensional model by structural homology for the rCPB2.8 protein was adjusted from Coelho *et al.*,³² with alteration in one of the structures used as a template, using the protein code PDB: 3I06 (1.10 Å) to replace the PDB: 2P7U (1.65 Å) used by the author. Then, a search was started for homologous proteins with a degree of sequential identity, obtained by the local alignment of known structures three-dimensionally, with the algorithm BLAST (Basic Local Alignment Search Tool).³³ A brief search for templates was also carried out using the online structural bioinformatics server MODBASE,³⁴ database of comparative models of protein structure and SWISSMODEL³⁵ dedicated

to homology modeling of 3D protein structures. Two crystallographic structures were selected (PDB: 3IUT, 1.2 Å and 3I06) present in the PDB database, which had good resolution, distribution of residues in the Ramachandran graph³⁶ and a good degree of identity and similarity.

Subsequently, comparative structural modeling was performed using the MODELLER²⁷ software version 9.16, with the construction of 100 models. The selection of the best model was carried out with the aid of the PROCHECK²⁸ program with analysis of the Ramachandran chart³⁶ and "G-factor".²⁸ The model was then validated using online software as Verify3D²⁹ and ProsaWeb,³⁰ in addition to the calculation of the RMSD (root-mean-square deviation) and then, optimized to obtain the proper structure for future molecular anchoring studies.

Molecular docking

Molecular docking analysis was performed using the Schrödinger software suite.³⁷ For ligand preparation, the LigPrep³⁸ program was used with OPLS_3 force field and ionization state for pH 7.0 ± 2.0 (using Epik). The protein structures preparation was realized by the Protein Preparation Wizard³⁹ program with the minimization performed using the OPLS-3 force field in the MacroModel⁴⁰ module.

For the docking analysis, the Induced Fit Docking (IFD)⁴¹ protocol was used, which performed the prediction of the protein structure and the refinement of the

compounds using the Prime⁴² program, as well as the docking and provides the score by the Glide⁴³ program, considering the protein and the ligand flexible. The grid box area was defined as 20 × 20 × 20 Å. The force field used was OPLS_3. The final ligand-protein complexes were visualized using the Maestro³⁷ version 11.1 (2017-1) interface, and figures were generated using its graphical interface and Pymol⁴⁴ software.

Chemistry

Melting points of compounds **2-4** were obtained via a Bücher 535 apparatus. Infrared (IR) spectroscopic analysis was performed using a Thermo Fisher Scientific Nicolet-iS50 spectrometer. Nuclear magnetic resonance (NMR) analysis was performed on a Bruker AC-300 (¹H: 300 MHz; ¹³C: 75 MHz) spectrometer. Mass spectroscopic analysis was conducted using XEVO-TQS (Waters Corporation) mass spectrometer equipment with ESI (electrospray) ionization font.

Synthesis of 5-(1-propenyl)-2H-1,3-benzodioxol (**1**)

The synthesis of compound **1** was performed according to the method described by Barreiro and Lima.⁴⁵ The procedure was conducted in a round bottom flask containing 1.0 g (6.172 mmol) of safrol and 5.0 mL of potassium hydroxide solution (KOH) 3 mol L⁻¹ in butyl alcohol (BuOH). The reaction mixture was kept under vigorous magnetic stirring and reflux at 110 °C for 6 h. The reaction was monitored by thin layer chromatography (TLC; hexane and ethyl acetate 9:1, v/v). After total consumption of the reactant, 15.0 mL of water were added at reaction and the pH of the aqueous phase was raised to approximately 7 by the addition of hydrochloric acid (HCl) solution (1 mol L⁻¹). The reaction mixture underwent extraction with ethyl acetate (3 × 20 mL), and the organic phase was dried with sodium sulfate anhydrous Na₂SO₄ and filtered. The solvent was removed by vacuum evaporation and the product purified by column chromatography (CC; ethyl acetate/hexane 5:95, v/v). Yellow oil; yield 77%; IR (KBr) ν / cm⁻¹ 3023, 2879, 1598, 1499, 1489, 1440, 1242, 1029; ¹H NMR (300 MHz, CDCl₃) δ 1.85 (d, 3H, *J* 6.4 Hz), 5.94 (s, 2H), 6.07 (dd, 1H, *J* 6.5, 15.6 Hz) 6.32 (dd, 1H, *J* 15.6 Hz), 6.74 (d, 2H, *J* 12.7 Hz), 6.89 (s, 1H); ¹³C NMR (75 MHz, CDCl₃) δ 18.4, 100.9, 105.3, 108.2, 120.0, 123.9, 130.5, 132.4, 145.5, 147.9.

Synthesis of 6-methyl-6,7-dihydro-2H,5H-indene[5,6-*d*][1,3]dioxol-5-one (**2**)

Compound **2** were synthesized as previously reported by Barreiro and Lima,⁴⁵ through Vilsmeier-Haack reaction. The procedure was conducted in a round bottom flask containing

0.35 mL (3.751 mmol) of phosphorus oxychloride (POCl₃) and 1.45 mL (18.869 mmol) of dry *N,N*-dimethylformamide (DMF). The reaction mixture was kept under vigorous magnetic stirring and an ice-bath immersion, at 0 °C for 30 min, in an atmosphere of argon. After this time was added 0.500 g (3.086 mmol) of isosafrol (**1**). The reaction was conducted at reflux in 110 °C for 6 h. The reaction was poured into 12.0 mL of ice and the pH was raised to 10 with sodium hydroxide 1 mol L⁻¹ NaOH_(aq), keeping under stirring for 12 h at room temperature. The reaction mixture underwent extraction with ethyl ether (3 × 15 mL); the organic phase was washed with saturated chloride sodium (NaCl) solution, dried over anhydrous Na₂SO₄, filtered and concentrated. The solvent was removed by vacuum evaporation and the product purified by column chromatography (CC; ethyl acetate/hexane 2:8, v/v). Orange solid; yield 62%; mp 61-65 °C; IR (KBr) ν / cm⁻¹ 2964, 2909, 1681, 1608, 1465, 1317, 1287, 1252, 1024; ¹H NMR (300 MHz, CDCl₃) δ 1.28 (d, 3H, *J* 7.3 Hz), 2.56-2.63 (dd, 1H, *J* 3.5, 16.8 Hz), 2.70 (m, 1H), 3.23-3.31 (dd, 1H, *J* 7.5, 16.9 Hz) 6.05 (s, 2H), 6.80 (s, 1H), 7.09 (s, 1H, H₆); ¹³C NMR (75 MHz, CDCl₃) δ 16.6, 34.9, 42.4, 102.1, 102.5, 105.6, 130.8, 148.2, 150.9, 154.2, 207.4.

Synthesis of 6,6-dimethyl-6,7-dihydro-2H,5H-indene[5,6-*d*][1,3]dioxol-5-one (**3**)

The synthesis of compound **3** was based on the methods described by Ranu and Jana.⁴⁶ Into a round bottom flask containing 0.4 g (4.000 mmol) of potassium *tert*-butoxide (*tert*-BuOK) solubilized at 7.5 mL of tetrahydrofuran (THF) previously dried, was added 0.250 g (1.315 mmol) of compound **2**, after 30 min, was added 0.3 mL (4.817 mmol) of iodomethane (CH₃I). The reaction mixture was left under vigorous magnetic stirring for 12 h at room temperature. After this time, the solvent (THF) was removed by vacuum evaporation, and a solid residue were solubilized in 9.0 mL of water. The pH was adjusted for 7 with 1 mol L⁻¹ HCl solution and extracted with ethyl acetate (3 × 10 mL). The organic phase was washed with saturated NaCl solution (1 × 5 mL), dried with anhydrous Na₂SO₄ and filtered. The solvent was removed by vacuum evaporation and the product purified by column chromatography (CC; ethyl acetate/hexane 2:8, v/v). Yellow solid; yield 75%; mp 69-72 °C; IR (KBr) ν / cm⁻¹ 2914, 1672, 1608, 1459, 1257, 1021; ¹H NMR (300 MHz, CDCl₃) δ 1.20 (s, 6H), 2.87 (s, 2H), 6.05 (s, 2H), 6.78 (s, 1H), 7.09 (s, 1H); ¹³C NMR (75 MHz, CDCl₃) δ 25.4, 42.8, 46.0, 102.1, 102.8, 105.7, 129.6, 148.2, 149.6, 154.3, 209.4.

Synthesis of *N*-[(5)-6,6-dimethyl-6,7-dihydro-2H,5H-indene[5,6-*d*][1,3]dioxol-5-ylidene] hydroxyl-amine (**4**)

The procedure to obtain compound **4** was based

and adapted according to the methodology reported by Gopalsamy.⁴⁷ In a round bottom flask containing 0.070 g (0.341 mmol) of compound **3**, 0.22 g of sodium acetate AcONa (2.683 mmol) and 0.19 g of hydroxylamine hydrochloride NH₂OH.HCl (2.714 mmol), 2.0 mL of methanol/water MeOH/H₂O (8:2, v/v) were added, with vigorous magnetic stirring at 65 °C for 48 h. Subsequently, 2.0 mL of water were added in reaction mixture and underwent extraction with dichloromethane (3 × 5 mL). The organic phase was dried over anhydrous Na₂SO₄, filtered and concentrated by vacuum evaporation and the product purified by column chromatography (CC; ethyl acetate/hexane 3:7, v/v). White solid; yield 55%; mp 77-79 °C; IR (KBr) ν / cm⁻¹ 3251, 2958, 2919, 1603, 1465, 1321, 1266, 1024, 930; ¹H NMR (300 MHz, CDCl₃) δ 1.32 (s, 6H), 2.83 (s, 2H), 6.00 (s, 2H), 6.71 (s, 1H), 7.94 (s, 2H); ¹³C NMR (75 MHz, CDCl₃) δ 28.4, 42.6, 45.9, 101.5, 105.3, 109.2, 126.0, 141.6, 146.8, 150.4, 165.0.

General procedure for the synthesis of derivatives **5a-5h**

The last stage of the synthetic route was the formation reaction of the series of oxime ethers (**5a-5h**) adapted from Li *et al.*⁴⁸ The procedure was conducted in a 50 mL round-bottom flask containing 15 mL of dimethylsulfoxide/water (8:2, v/v), 0.600 g of potassium hydroxide (0.107 mmol, 13 equivalents) and 0.150 g of derivative **4** (0.83 mmol, 1 equivalent). The mixture was under magnetic stirring at room temperature for 30 min. Then, 2 equivalents of the corresponding benzyl halide were added. The reaction continued for approximately 30 min, when the total consumption of the starting material was observed by thin layer chromatography (eluent: hexane/ethyl acetate, 6:4, v/v). Then, 30.0 mL of saturated NaCl solution was added to the flask containing the mixture and transferred to a 100 mL separating funnel. The organic phase was obtained by extraction with ethyl acetate (4 × 20 mL), and then washed with distilled water (2 × 20 mL), dried with Na₂SO₄, filtered and concentrated on a rotary evaporator under reduced pressure. The product obtained was subjected to purification by silica column chromatography (ethyl acetate/hexane, 95:5, v/v).

6,6-Dimethyl-6,7-dihydro-5*H*-indene[5,6-*d*][1,3]dioxol-5-one *O*-(4-methoxybenzyl) oxime (**5a**)

White oil; yield 65%; IR (KBr) ν / cm⁻¹ 2954, 1603, 1262, 1237, 1029, 941; ¹H NMR (300 MHz, CDCl₃) δ 1.32 (s, 6H), 2.79 (s, 2H), 3.81 (s, 3H), 5.11 (s, 2H), 5.95 (s, 2H), 6.68 (s, 1H), 6.89 (d, 2H, *J* 8.5 Hz), 7.36 (d, 2H, *J* 8.5 Hz), 7.73 (s, 1H); ¹³C NMR (75 MHz, CDCl₃) δ 28.5, 42.6, 45.8, 55.2, 76.1, 101.4, 105.2, 109.1, 113.6, 126.3, 129.8, 130.1,

141.5, 146.5, 150.1, 159.1, 164.5; MS (ESI) *m/z*, calcd. for C₂₀H₂₁NO₄ [M + H]⁺: 340.39, found: 340.53.

6,6-Dimethyl-6,7-dihydro-5*H*-indene[5,6-*d*][1,3]dioxol-5-one *O*-(4-*tert*-butylbenzyl) oxime (**5b**)

White oil; yield 31%; IR (KBr) ν / cm⁻¹ 2954, 1608, 1465, 1262, 1034, 1009; ¹H NMR (300 MHz, CDCl₃) δ 1.32 (s, 6H), 1.35 (s, 9H), 2.81 (s, 2H), 5.18 (s, 2H), 5.97 (s, 2H), 6.70 (s, 1H), 7.40 (s, 4H), 7.80 (s, 1H); ¹³C NMR (75 MHz, CDCl₃) δ 28.5, 31.4, 34.9, 42.6, 45.9, 76.3, 101.4, 105.3, 109.2, 125.2, 126.4, 127.9, 135.1, 141.5, 146.6, 150.1, 150.5, 164.5; MS (ESI) *m/z*, calcd. for C₂₃H₂₇NO₃ [M + H]⁺: 366.47, found: 366.35.

6,6-Dimethyl-6,7-dihydro-5*H*-indene[5,6-*d*][1,3]dioxol-5-one *O*-(4-bromobenzyl) oxime (**5c**)

White oil; yield 21%; IR (KBr) ν / cm⁻¹ 2914, 1603, 1470, 1266, 1034, 1005; ¹H NMR (300 MHz, CDCl₃) δ 1.26 (s, 6H), 2.80 (s, 2H), 5.13 (s, 2H), 5.97 (s, 2H), 6.69 (s, 1H), 7.23 (d, 2H, *J* 8.4 Hz), 7.29 (d, 2H, *J* 8.4 Hz), 7.75 (s, 1H); ¹³C NMR (75 MHz, CDCl₃) δ 28.5, 42.7, 45.8, 75.5, 101.5, 105.3, 109.0, 121.6, 126.2, 129.3, 131.5, 137.0, 141.7, 146.7, 150.3, 165.0; MS (ESI) *m/z*, calcd. for C₁₉H₁₈BrNO₃ [M + H]⁺: 389.26, found: 389.34.

6,6-Dimethyl-6,7-dihydro-5*H*-indene[5,6-*d*][1,3]dioxol-5-one *O*-(4-fluorobenzyl) oxime (**5d**)

Yellow oil; yield 27%; IR (KBr) ν / cm⁻¹ 2919, 1603, 1510, 1465, 1262, 1034; ¹H NMR (300 MHz, CDCl₃) δ 1.28 (s, 6H), 2.79 (s, 2H), 5.14 (s, 2H), 5.96 (s, 2H), 6.69 (s, 1H), 7.03 (t, 2H, *J* 8.5 Hz), 7.39 (dd, 2H, *J* 5.5, 8.31 Hz), 7.74 (s, 1H); ¹³C NMR (75 MHz, CDCl₃) δ 28.5, 42.7, 45.8, 75.6, 101.4, 105.3, 109.0, 115.0, 115.2, 126.2, 129.6, 129.9, 134.0, 141.7, 146.6, 150.2, 160.7, 163.9, 164.9; MS (ESI) *m/z*, calcd. for C₁₉H₁₈FNO₃ [M + H]⁺: 328.35, found: 328.39.

6,6-Dimethyl-6,7-dihydro-5*H*-indene[5,6-*d*][1,3]dioxol-5-one *O*-(4-methylbenzyl) oxime (**5e**)

Yellow oil; yield 33%; IR (KBr) ν / cm⁻¹ 2919, 1900, 1603, 1465, 1262, 1034; ¹H NMR (300 MHz, CDCl₃) δ 1.29 (s, 6H), 2.36 (s, 3H), 2.80 (s, 2H), 5.15 (s, 2H), 5.96 (s, 2H), 6.68 (s, 1H), 7.16 (d, 2H, *J* 7.8 Hz), 7.32 (d, 2H, *J* 7.9 Hz), 7.76 (s, 1H); ¹³C NMR (75 MHz, CDCl₃) δ 21.2, 28.5, 42.6, 45.9, 76.3, 101.4, 105.2, 109.2, 126.3, 128.2, 129.0, 135.0, 137.3, 141.5, 146.6, 150.1, 164.5.

6,6-Dimethyl-6,7-dihydro-5*H*-indene[5,6-*d*][1,3]dioxol-5-one *O*-(4-(trifluoromethyl)benzyl) oxime (**5f**)

Yellow oil; yield 33%; IR (KBr) ν / cm⁻¹ 2919, 1465, 1317, 1266, 1058; ¹H NMR (300 MHz, CDCl₃) δ 1.27 (s,

6H), 2.80 (s, 2H), 5.24 (s, 2H), 5.98 (s, 2H), 6.70 (s, 1H), 7.51 (d, 2H, *J* 8.1 Hz), 7.60 (d, 2H, *J* 7.9 Hz), 7.77 (s, 1H); ¹³C NMR (75 MHz, CDCl₃) δ 28.4, 42.7, 45.8, 75.3, 101.5, 105.4, 109.0, 125.2, 125.2, 125.4, 126.1, 127.6, 127.8, 141.8, 142.5, 146.7, 150.4, 165.2.

6,6-Dimethyl-6,7-dihydro-5*H*-indene[5,6-*d*][1,3]dioxol-5-one *O*-(4-chlorobenzyl) oxime (**5g**)

White oil; yield 22%; IR (KBr) ν / cm⁻¹ 2860, 1900, 1465, 1262, 1079, 797; ¹H NMR (300 MHz, CDCl₃) δ 1.28 (s, 6H), 2.80 (s, 2H), 5.15 (s, 2H), 5.97 (s, 2H), 6.70 (s, 1H), 7.28 (d, 2H, *J* 8.4 Hz), 7.33 (d, 2H, *J* 8.4 Hz), 7.76 (s, 1H); ¹³C NMR (75 MHz, CDCl₃) δ 28.5, 42.7, 45.8, 75.4, 101.5, 105.3, 109.0, 126.2, 128.6, 129.0, 133.4, 136.5, 141.7, 146.7, 150.3, 165.0.

6,6-Dimethyl-6,7-dihydro-5*H*-indene[5,6-*d*][1,3]dioxol-5-one *O*-(4-nitrobenzyl) oxime (**5h**)

Yellow oil; yield 46%; IR (KBr) ν / cm⁻¹ 2914, 1603, 1514, 1336, 1262, 1034; ¹H NMR (300 MHz, CDCl₃) δ 1.25 (s, 6H), 2.80 (s, 2H), 5.29 (s, 2H), 5.99 (s, 2H), 6.71 (s, 1H), 7.53 (d, 2H, *J* 8.4 Hz), 7.76 (s, 1H), 8.19 (d, 2H, *J* 8.6 Hz); ¹³C NMR (75 MHz, CDCl₃) δ 28.4, 42.8, 45.8, 74.8, 101.6, 105.4, 108.9, 123.5, 126.0, 128.0, 142.0, 146.3, 146.8, 147.2, 150.5, 165.7.

Results and Discussion

The choice of enzyme targets was based on some factors, as their importance for the parasite's feasibility; the absence of similar structures in humans, and the similarity of functional groups of known drugs interacting with the selected enzyme classes. In turn, the proposed changes in the molecules are related to drugs and patents already registered with proven leishmanicidal activities.²⁴⁻²⁶ The variations include: changes in water solubility; the addition of bulky groups; addition of electron donating groups to the aromatic ring and electron withdrawers; acceptor groups and donors of hydrogen interactions.

Surwase *et al.*⁴⁹ recently have published a study in which they obtained oximic derivatives as a potent leishmanicidal agent with structural patterns similar to the oxime ethers studied. Considering different types of biological activity that oximic and oxydic derivatives can present, including protozoicide, these substances are a good choice for the development of new drug candidates, including leishmanicides. In addition to the planned molecule presenting portions, in the case of rCPB2.8, the literature shows its affinity for substrates of basic character, a characteristic found in the compounds of the series by the presence of nitrogen from the oximic ether; and in CRK3

by substrates with hydrophobic moieties, as *para*-substituted aromatic and methyl moieties.^{25,50} It was according to the promising results of modeling studies with the selected molecules that the next synthetic step was taken in order to evaluate their activity in the future *in vitro* and *in vivo* studies.

Homology modeling

The prediction model of the three-dimensional structure of the CRK3 protein based on Pereira *et al.*,¹⁵ presented good stereochemical quality, with 91.4% of waste in favorable regions, 7.0% in permitted regions and 0.8% in unfavorable regions in the Ramachandran graph, very similar to what the study reported (Figure 2a). In addition to a RMSD of 0.367 Å when aligned with the PDB code template structure: 2R3I (Figure 2b).

The rCPB2.8 enzyme was validated by other methods since the mold structures were not used in a previous study. With a satisfactory modeling result, it showed 93.9% of its residues in favorable regions and 0% in regions that are not allowed in the Ramachandran graph (Figure 2c). The results obtained by Verify3D, which assigns a structural class based on the location and environment of each position of amino acid residues, comparing the results obtained with good structures, demonstrated that most of the values obtained are within the acceptable range (0.16 and 0.8), and 92.56% of the residues have an average 3D-1D score greater than 0.2, a value to which it can be assumed that the structural folding of the built model is reliable. In addition to an RMSD of 0.328 Å when compared to one of the mold structures, of better resolution, with PDB code 3I06 (Figure 2d).

Molecular docking

The molecular docking studies were carried out with the proposed series of oximic chemical derivatives and the two modeled enzymes, CRK3 and rCPB2.8, after an analysis of the physicochemical properties of the ligands in relation to their ADMET (absorption, distribution, metabolism, and excretion) properties and agreement with the Lipinski parameters.⁵¹ The compounds showed results of desirable physicochemical properties in theoretical studies, pointing out good solubility and permeability in membranes by oral administration.

rCPB2.8

From the connection energy results obtained by docking, expressed through Table 1, the pentamidine drug, second choice for the treatment of leishmaniasis, showed a better value than all the ligands, including the cruzain protease cysteine inhibitor (QL2).

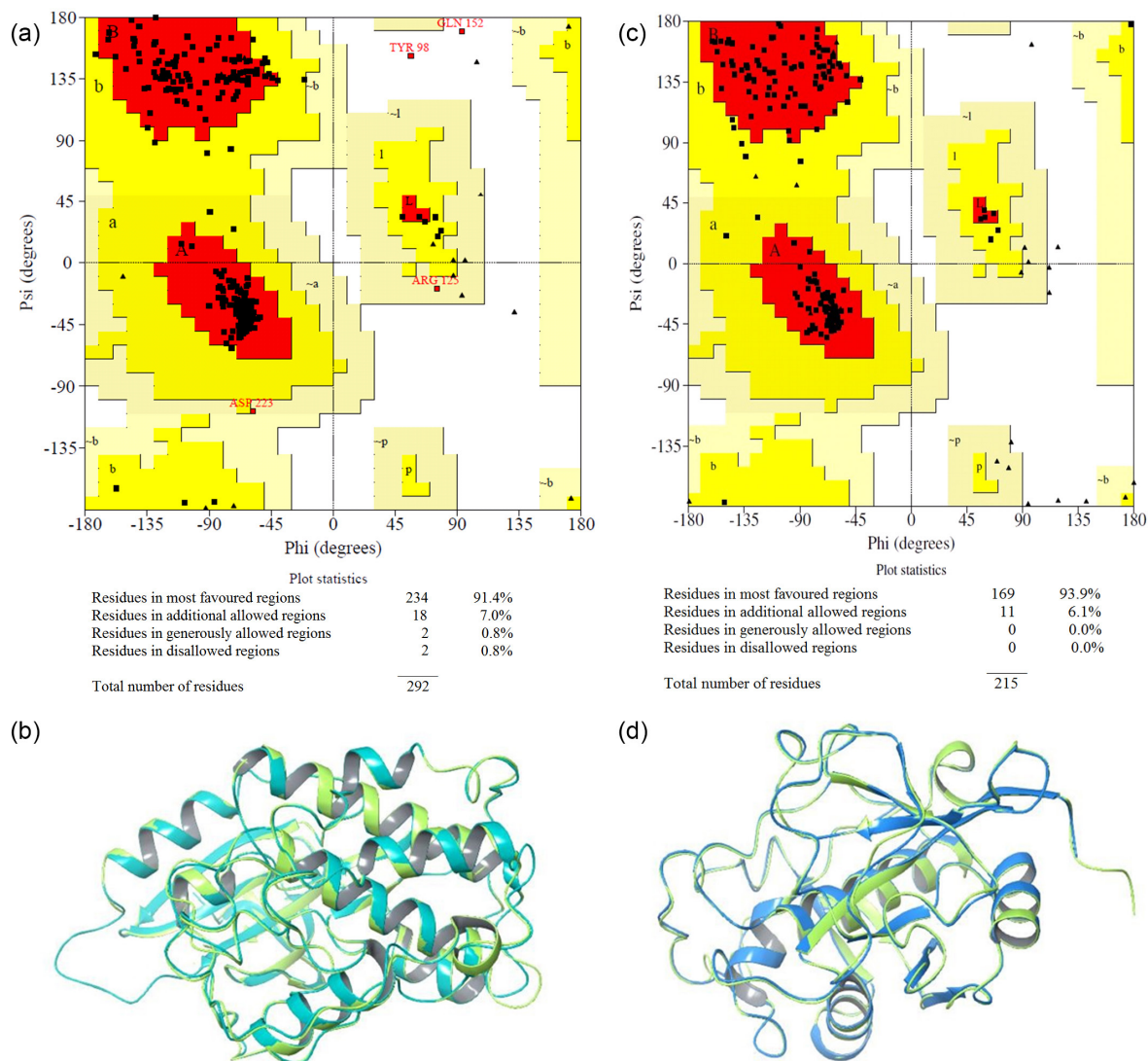


Figure 2. Model quality validation. (a) Ramachandran plot of CRK3 enzyme; (b) superposition of the homology model of CRK3 with the structure of CDC human used as template (PDB code: 2R31); (c) Ramachandran plot of rCPB2.8 enzyme; (d) superposition of the homology model of rCPB 2.8 with the structure of cruzain used as template (PDB code: 3I06).

Table 1. Binding energies, represented as Glide Score, type and amino acids interactions, calculated by the IFD^a protocol (Schrodinger) program at all ligands and the rCPB2.8 protein

Ligand	Binding energies / (kcal mol ⁻¹)			
	GlideScore	H bond ^b	aa ^c	Good interactions (vdW) ^d
Pentamidine	-7.521	4	ASP21, ASP67, ASP191	206
5g	-6.515	0		242
5c	-6.461	0		261
Inhibitor QL2 ^e	-6.422	1	GLN22	158
5f	-6.365	0		290
5d	-6.329	1	TRP188	232
5a	-5.919	3	GLN22, GLY23, TRP192	218
5b	-5.609	2	GLY23, TRP192	227
5h	-5.440	1	GLY23	191
5e	-5.200	0		224

^aInduced fit docking; ^bhydrogen bond; ^camino acids; ^dvan der Waals; ^erCPB2.8 inhibitor.

The ligands with two electronegative substituents **5g** (chlorine) and **5c** (bromine), however, showed a better interaction value than the QL2 inhibitor, with a purine base replaced by a ring linked to two fluorine atoms and one nitrile, from one of the molds used (PDB: 3I06). Although they did not present any hydrogen bond with the target enzyme, which characterizes a strong bond, these compounds are characterized by having groups removing electrons from the aromatic ring, enabling π -stacking interaction between this aromatic ring and the electron-rich aromatic ring of the TRP188 (tryptophan) and TRP192. TRP188 is part of the substrate's interaction, close to the active site of the cysteine proteases called S1' together with GLN22, a residue that showed hydrogen bonding with the inhibitor. Along with that, they had a greater number of good interactions, followed only by the compound **5f**.

Most compounds showed π -stacking interaction with TRP188. In 2018, Coelho *et al.*³² obtained molecules with expressive activity *in vitro* against *Leishmania*, and the highest of them had the same type of interaction, with the same catalytic residue.

Compound **5a** with a methoxy as a substituent, presented an interaction profile similar to that of the inhibitor with the residue of GLN22, an amino acid with an uncharged polar side chain containing an amide group, which acts as a receptor group for the interaction of hydrogen and nitrogen of the oximic ether of the proposed ligand as well as the inhibitor nitrile nitrogen. Although the rCPB2.8 enzyme has a high affinity for compounds of basic character, the only compound that allowed the interaction between the nitrogen of the oximic ether closest to this profile was **5a**, with an average energy value among the others.

A successful covalent inhibitor of cysteine proteases in their pre-reactive form must first be able to fit non-covalently to the enzyme binding site in order to bring the electrophilic center closer to the sulfur atom of cysteine, a residue of catalytic triad. Non-covalent binding interactions, as hydrogen bonds, hydrophobic, ionic interactions, van der Waals and de-solvation processes, are responsible and important for the correct binding of the ligand. Molecular modeling routinely addresses these non-covalent contributions to ligand binding without considering the contribution of the covalent reaction.⁵²

In a comparison with a previous study⁵³ to this coupling study, the potential for a possible formation of a covalent bond was determined for the best binding pose of the three highest-value ligands of GlideScore and pentamidine by measuring the distance between the nucleophilic sulfur atom of the active site cysteine residue and the electrophilic atoms of the ligand and other possible ones responsible for this type of interaction. The expected connection modes

with a distance of less than 5.00 Å were interpreted as possible initial geometry for covalent bond formation as described by Fey *et al.*⁵³ In addition to them, good van der Waals interactions between the ligand and the residue were also considered.

Although none of the proposed ligands have shown an interaction of hydrogen, which is characterized by being stronger than the others, and of no other type directly with the catalytic triad of the enzyme, cysteine/asparagine/histidine (CYS, ASN, HIS) and, since the inhibitor QL2 presents a covalent bond between the sulfur of CYS25 (ref. CYS28 mold) and its nitrile carbon, these measures were compared in order to predict whether a possible interaction could occur by predicting whether the ligands could express an activity in subsequent leishmanicidal activity tests.

The compound **5g** showed a distance of 4.07 Å between the sulfur of the cysteine and the oxygen atom of the methylenedioxi group of safrol and 4.81 Å with the carbon atom of the same group, in addition to presenting three types of good interaction of van der Waals between these atoms (Figure 3c). Pentamidine, on the other hand, besides not showing any kind of good van der Waals interaction, kept the distances between the sulfur and its atoms above 5.00 Å (Figure 3a). The same happened with compound **5f**.

The ligand replaced with bromine (**5c**) was the one with the shortest bonding distance between sulfur and oxygen in its ring with a value of 3.70 and 4.11 Å, respectively, with methylene carbon (Figure 3b) in addition to being responsible for five good interactions with the residue, a distance very close to that of the covalent bond performed from the redocking of the 3.57 Å QL2 inhibitor.

When comparing the results obtained by the current study with Fey *et al.*,⁵³ such distances demonstrate a more promising value than that obtained by them, in which, as well as Coelho *et al.*,³² also presented aziridine molecules with satisfactory inhibitory activity for the *Leishmania*. Based on results obtained by de Luca *et al.*,⁵⁴ the distance between the residues and electronegative atoms of the benzimidazole series is similar with the best results of the half maximal inhibitory concentration IC₅₀ (µM) against the parasite, with values around 0.4, 0.5 and 0.6 µM.

Based on the result obtained, it is possible to predict that the proposed ligands have a high capacity to present expressive activities against the parasite. The analysis of the results also shows that the presence of an electron withdrawing substituent has a better bonding profile than donors, which had already been established through the study of the structure × activity relationship by Mott *et al.*,²⁴ when resolving the structure of the CPB inhibitor and analogues (PDB 3I06).

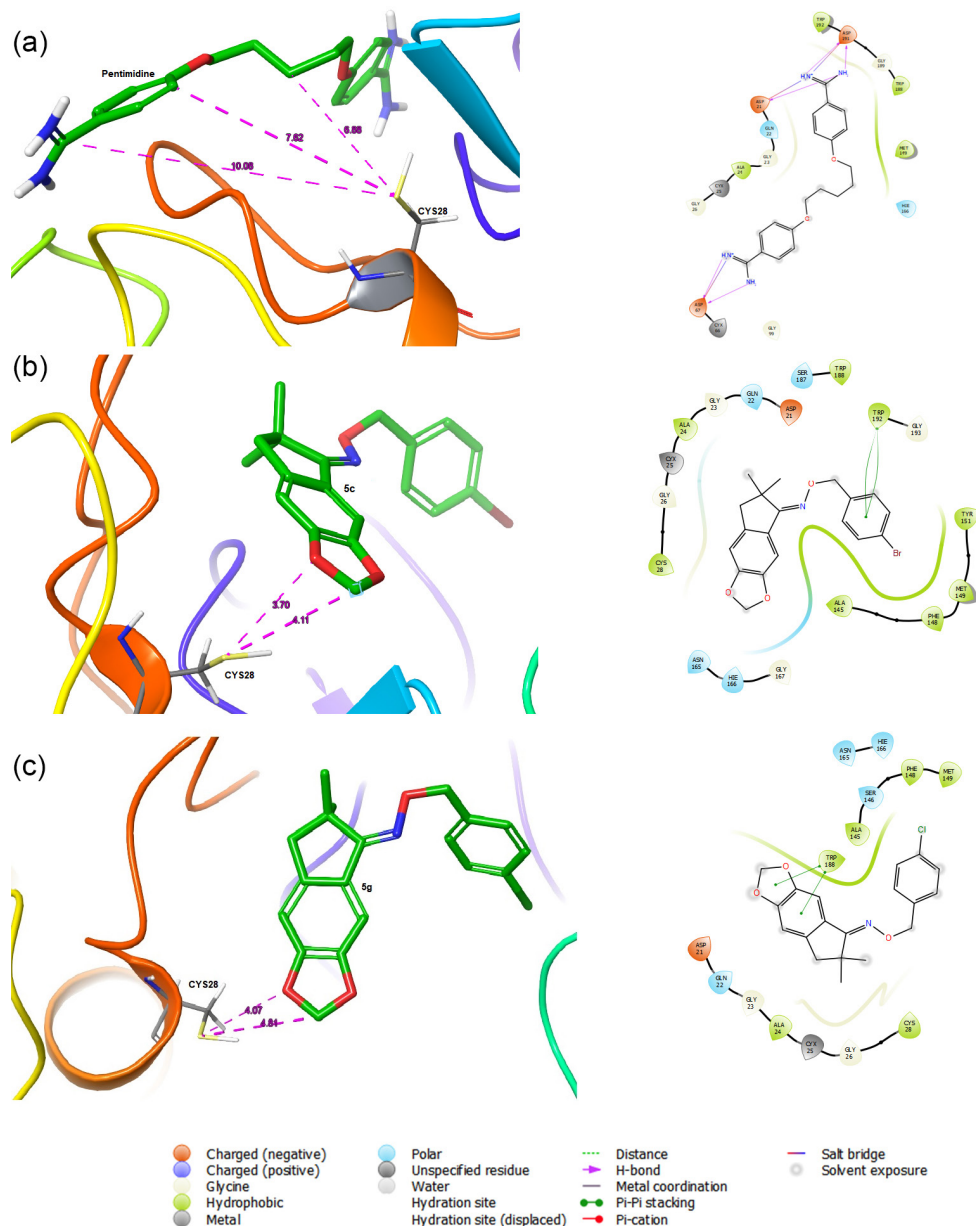


Figure 3. 3D structure representing the distance between the atoms that could participate to the possible covalent interaction between protein and ligand (purple dotted line), and 2D scheme demonstrating interactions between residues of the enzyme and the compounds (a) pentamidine, (b) **5c** and (c) **5g**.

CRK3 and CDK2

The cyclin-dependent kinase inhibitor (SCF) is known to inhibit the human CDK2 enzyme, present in the crystallographic structure co-crystallized with this enzyme (PDB code: 2R31), was studied to evaluate its affinity with the CRK3 enzyme of *Leishmania*, due to the similarity between the two enzymes (Table 2).

Likewise, with the purpose of avoiding undesirable adverse effects due to the possibility of low selectivity of the proposed compounds with the target enzyme in relation to the human enzyme, since the CRK3 enzymes of *Leishmania* and human CDK2 have approximately

57% identity, we sought to verify the affinity between the proposed molecules and the human enzyme by molecular anchoring studies (Table 3).

Considering the results illustrated in Tables 2 and 3, with respect to the CRK3 enzyme, we were able to observe that pentamidine obtained a lower GlideScore value when compared to some of the analyzed compounds. In turn, the inhibitor (SCF) was the molecule that had the greatest affinity with the enzyme. Both in the enzyme CDK2 and in CRK3, the inhibitor resolved with it, obtained a value well above that of the drug. Pentamidine, on the other hand, showed in the CRK3 molecule strong interactions, of hydrogen, with amino acids of the active site valine

Table 2. Binding energies represented as GlideScore, type and amino acids interactions, calculated by the IFD^a protocol (Schrödinger) program at all ligands and the CRK3 protein

Ligand	Binding energies / (kcal mol ⁻¹)			
	GlideScore	H bond ^b	aa ^c	Good interactions (vdW) ^d
Inhibitor SCF ^e	-9.562	3	LYS33, VAL83	346
5f	-8.666	2	LYS33, VAL83	358
5h	-8.588	1	LYS33	371
5a	-8.517	2	LYS33, VAL83	413
5d	-8.355	1	LYS88	378
Pentamidine	-8.064	6	GLU12, VAL83, GLU84, ASP86, GLU161	324
5c	-8.061	0		384
5g	-7.437	0		330
5b	-6.839	2	TYR82, LYS89	297
5e	-6.772	1	ASN131	244

^aInduced fit docking; ^bhydrogen bond; ^camino acids; ^dvan der Waals; ^eCRK3 inhibitor.

Table 3. Binding energies, represented as GlideScore, type and amino acids interactions, calculated by the IFD^a protocol (Schrödinger) program at all ligands and the CDK2 protein

Ligand	Binding energies / (kcal mol ⁻¹)			
	GlideScore	H bond ^b	aa ^c	Good interactions (vdW) ^d
Inhibitor SCF ^e	-10.376	3	GLU8, LEU83	307
5a	-8.533	0		390
5d	-8.318	1	LEU83	332
5e	-7.865	1	LYS89	324
Pentamidine	-7.813	6	GLU12, LYS89, ASP145, GLU162	261
5f	-7.739	1	LYS89	323
5g	-7.203	0		302
5c	-6.732	0		298
5b	-6.274	0		356
5h	-6.109	2	LYS129, ASN132	310

^aInduced fit docking; ^bhydrogen bond; ^camino acids; ^dvan der Waals; ^eCDK inhibitor.

and asparagine (VAL83 and ASP86), different from the interactions presented by the human enzyme, which can establish a higher selectivity for the protozoan enzyme, since it is a second choice drugs currently used. However, even in the human enzyme (CDK), the drug was the one with the highest number of hydrogen interactions between amino acids, which may explain its high toxicity.

The three molecules with the highest GlideScore value in the *Leishmania* enzyme were **5f**, **5h** and **5a** (Figure 4), all of which showed hydrogen interaction with lysine LYS33, belonging to the active site of the protein, besides two of them (**5f** and **5a**) also interacting with VAL83, similar to the enzyme inhibitor and, residue that corresponds to the portion of hinge present in the active site of cyclin-dependent enzyme kinases.⁵⁰ When compared to the human enzyme, the molecule bearing a

nitro group as a substitute for the oximic ether is the most important ligand promising for the protozoan enzyme, since in CDK2 it was the molecule that had the lowest GlideScore value. This compound is characterized by having an electronegative group, which removes electrons from the aromatic ring, enabling the π -stacking interaction between this aromatic ring and the PHE80 electron-rich aromatic ring.

The **5a** molecule, although with a high interaction value in CRK3, also showed a high value in the human enzyme and a greater number of good interactions of van der Waals in both, showing that the search for a specific molecule for the parasite should have a more discerning approach. According to the values obtained, the presence of a large group of electron donors in the *para*-disubstituted aromatic ring resulted in the worsening of the interaction profile

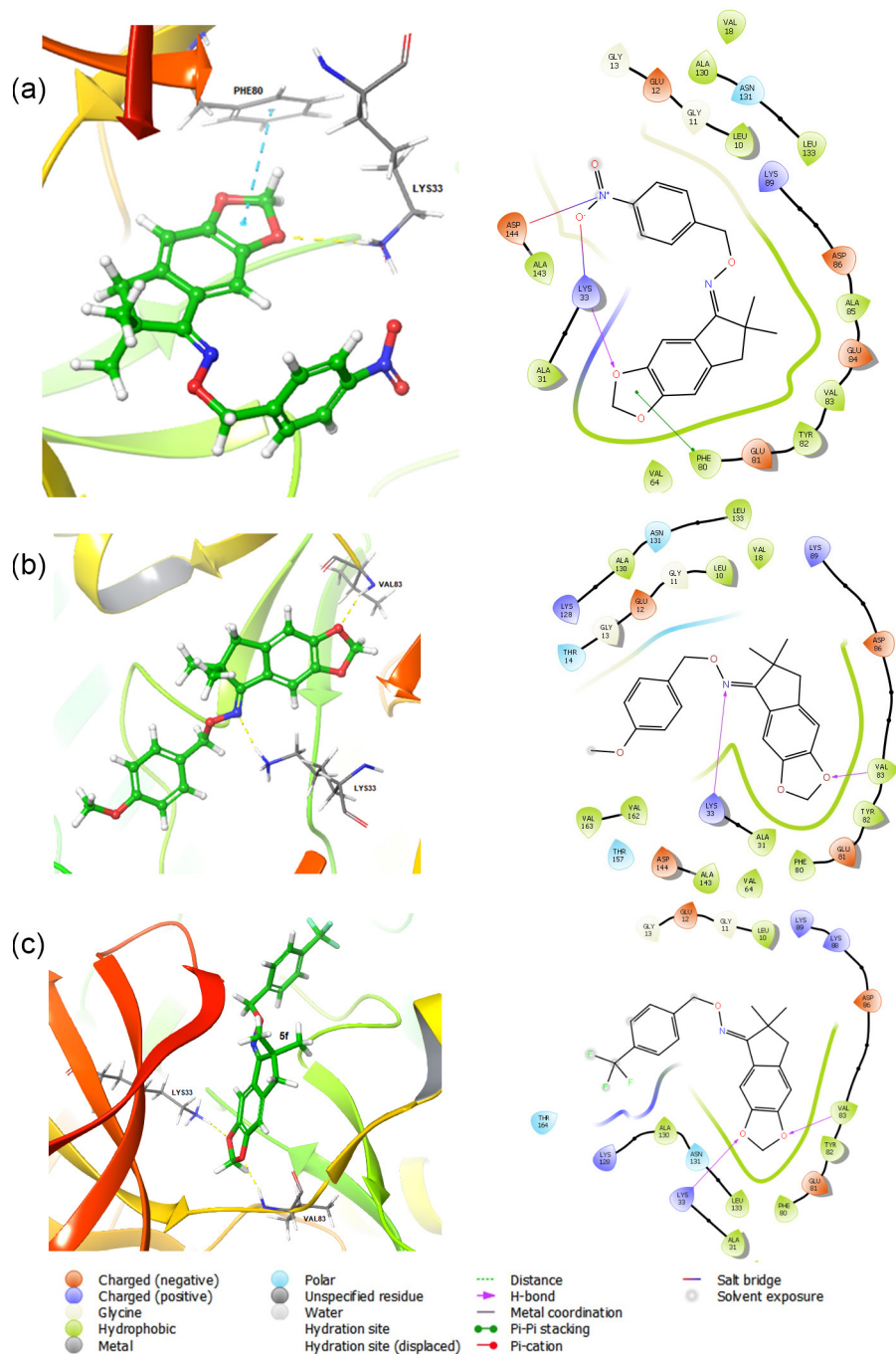


Figure 4. 3D structure representing the hydrogen bond (yellow dotted line) and π - π stacking (blue dotted line) between protein and ligand, and 2D scheme demonstrating interactions between residues of the enzyme and the compounds (a) **5h**, (b) **5a** and (c) **5f**.

between CRK3 and the compounds, giving molecules **5b** and **5e** a lower GlideScore value, with the exception of **5a** that carried the methoxy in that position.

Most of the interactions between the oximic ethers and the CRK3 enzyme occurred mainly in the oxygen of methylenedioxy and, in the case of the **5a** molecule, with the oximic nitrogen demonstrating a good choice of the molecule's skeleton, which can provide strong hydrogen bonds.

The molecule bearing a fluorine (**5d**) showed an interaction of hydrogen with leucine LEU83, an amino acid that in the *Leishmania* enzyme changes to VAL83 and, because they present this interaction profile, do not demonstrate molecules that can be selective in this case, since both the valine, as for leucine, are nonpolar and neutrally charged amino acids. It is worth mentioning that the compound **5a** that presented the lowest binding energy value followed only by its inhibitor in the human enzyme,

can also be an alternative to be studied, for other purposes, since the CDK has a crucial role in the regulation of the division cell and its abnormal activity is closely related to several types of cancer. A selective inhibitor of the human enzyme may be a prototype proposal to drug in cases like that.⁵⁵

The comparison between the molecules and studies done so far, gives us a good expectation about the ligands, since it was possible to achieve success in homology modeling of the enzyme when comparing the amino acid chains between them.

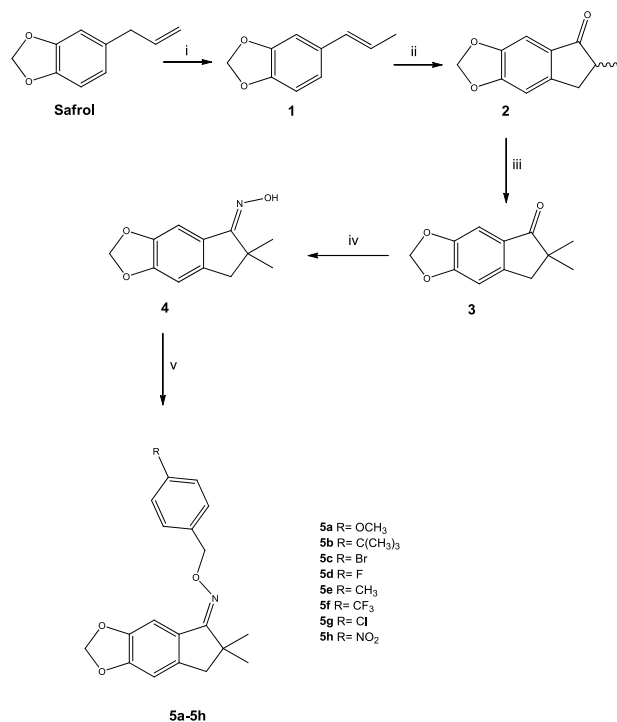
It is necessary to carry out toxicity studies with the proposed compounds in relation to their affinity for the enzyme CDK2, but the molecular anchoring tools would allow the study and planning of substances with greater selectivity by the CRK3 enzyme of *Leishmania* and less probable toxicity due to interaction with the CDK2 enzyme, as of studies of the different amino acid residues present in the active site of the CRK3 enzyme and which are not found in the human enzyme.

Based on the results obtained, the synthetic step of the oxyme derivatives presented below was performed.

Chemistry

The synthetic route used for obtention of oximic ethers of safrol (**5a-5h**), is represented in Scheme 1. The first step (i) consists of the isomerization of the starting product (safrol) generating compound **1**. Then, it goes through the Vilsmeier Haack reaction (step ii), forming and cyclizing the previous molecule, generating an indanone (**2**), which has an asymmetric center. Aiming to eliminate it and make the structure simpler stereochemically, a C-alkylation reaction is performed, adding a methyl to the carbon α adjacent to the carbonyl (step iii). The product generated (**3**) is subjected to an addition reaction with hydroxylamine hydrochloride in basic medium (step iv) producing the oxy-chemical intermediate **4**. Then, this intermediate will be subjected to reaction with benzyl halides (step v) forming the new series of derivatives of oximic ethers (**5a-5h**).

The product of the isomerization of the double bond in the side chain of the aromatic ring of safrol (**1**), presented itself in a thermodynamically stable form, after purification. As observed in the ¹H NMR spectrum, the alkene isomerization of the safrol molecule was confirmed by the presence of a doublet at 1.85 ppm (*J* 6.4 Hz) attributed to the hydrogen of the terminal methyl of the isosafrol. At 6.0 ppm (dd, 1H, *J* 6.5, 15.7 Hz) and 6.3 ppm (dd, 1H, *J* 15.6 Hz) there were signs attributed to the vinyl hydrogen, confirmed by the coupling constants, which confirms the link between the hydrogen of the allylic chain and, due to



Scheme 1. General scheme used for the preparation of oximic ethers. Reagents, conditions and yields: (i) KOH/*n*BuOH (3 mol L⁻¹), 120 °C, 3 h, (yield 77%). (ii) POCl₃, DMF, argon, 110 °C, 6 h, (yield 62%). (iii) THF, CH₃I, *tert*-BuOK, argon, 12 h, rt (yield 75%). (iv) NH₂OH.HCl, AcONa, MeOH/H₂O, 65 °C, 48 h (yield 55%). (v) Benzyl halides, DMSO/H₂O, KOH, (variable time and yield).

their lower displacements, close to 6.00 ppm, points out that the molecule (**1**) assumes the *cis* conformation.⁵⁶

Compound **2** was obtained by forming a cyclopentanone substituted with methyl from DMF and phosphorus oxychloride (POCl₃), subsequent to a cyclization step, through the Vilsmeier-Haack reaction. Through the “one pot” reaction, the first step consists of the formulation of the aromatic ring with subsequent cyclization, aiming to obtain an indanone adjacent to the aromatic ring of the starting product (**1**). The certainty of obtaining the product was the band C=O in 1681 cm⁻¹ in the IR spectrum and the appearance of the carbon signal of ketone carbonyl in 207.4 ppm.

The next step was the elimination of the asymmetric center of the indanone methyl by means of C-alkylation (**3**). α -Carbonyl hydrogen was replaced by the methyl group by means of a bimolecular nucleophilic substitution (S_N2). Then, the key step for the formation of the ethers was to obtain the oxy-intermediate (**4**), which consisted of the conversion of the carbonyl (R-C=O) by an oxime (R-C=N-OH), from the reaction with hydroxylamine hydrochloride (NH₂OH.HCl) in hydromethanolic solution in the presence of sodium acetate, a basic salt that has the purpose of favoring the nucleophilic attack of hydroxylamine to carbonyl carbon so that the reaction

of nucleophilic addition with the production of oximic diastereoisomers (*E/Z*). The confirmation took place with the band in the hydroxyl region in 3251 cm^{-1} and the absence of the carbon signal of the ketone carbonyl close to 209.0 ppm and the presence of a signal at 165.0 ppm , demonstrating its substitution by an imine, characteristic in this region.

The final stage of obtaining the oxime ether series (**5a-5h**), through coupling reactions with their respective substituted benzyl halides, were confirmed by the disappearance of the band O–H (3251 cm^{-1}) and, in the NMR spectrum of ^1H the main spectroscopic characteristics observed were the appearance of a signal in the regions between 5.0 and 5.2 ppm , referring to the hydrogen of the ether functions of oximes ($\text{C}=\text{N}-\text{O}-\text{CH}_2$). In the NMR spectra of ^{13}C , the appearance of signals in the region of 75.0 to 76.0 ppm refers to the carbons of the same functional group ($\text{C}=\text{N}-\text{O}-\text{CH}_2$). The signal close to 1.3 ppm matches to the hydrogens of the geminal-methyls from carbon α to carbonyl, and at 2.8 ppm to the adjacent methylenes. Methylene dioxy is represented by signals close to 6.0 ppm in the ^1H and 101.4 ppm in the ^{13}C spectrum, like imine's carbon ($\text{C}=\text{N}$) at 165.0 ppm . Furthermore, with the H4 displacement remaining close to 8.0 ppm , the products were characterized as the *Z* isomer. An AA'BB' system, two doublets, with coupling values of approximately 8.5 Hz was also observed in the aromatics region, showing the presence of aromatic rings *p*-disubstituides replaced. In 2019, Silva *et al.*⁵⁷ synthesized analogues of oxime ethers similar to the described here, from vanillin, which showed analgesic and anti-inflammatory activities; in the study the authors obtained a mixture of isomers of the oxime derivatives in which the *E* isomers had an H4 displacement closer to 7.0 and 7.9 ppm for *Z* isomer.⁵⁷

Conclusions

Through the molecular modeling studies carried out, it was possible to validate the enzyme targets chosen as promising targets for the studies of prototypes to leishmanicidal drugs, which can lead to equivalent results in subsequent pharmacological studies *in vitro* studies. The results obtained by molecular anchoring allowed us to infer that the proposed series of substances may present a promising leishmanicidal profile as inhibitors of the studied enzymes and may prompt the development of a new series of related inhibitors and object of new studies of biological activity.

The presence of the methylenedioxy and oxyhemic group was essential for interaction between the compounds of the series and the enzymes CRK3 and rCPB2.8 in molecular anchorage studies. In the rCPB2.8 enzyme,

compounds containing electron donating clusters to the aromatic ring *p*-disubstituted by the resonance effect showed a leishmanicidal activity of slightly greater magnitude than those containing electron withdrawing clusters due to the increase in the electronic density in this ring and enabling a stronger interaction like π -stacking and cation- π . This happened with the molecules of greater ligand-receptor interaction, with substituents as chlorine (**5g**) and bromine (**5c**), and of the interaction between the electrons in the aromatic ring of the ligand and the amino acids TRP188 and TRP192 since such amino acids are part of one of the sub-sites of interaction with the substrate and close to the active site of cysteine proteases. In addition, the distances between atoms possible to make a covalent bond of the molecule of interest and the residue of CYS28 (equivalent to the CYS25 of the mold), part of the catalytic site of the enzyme, also presents the possibility of formation of this type of bond, which would be essential for enzyme inhibitory activity.

In the CRK3 enzyme, obtaining binding energy values of three of the synthesized compounds **5a**, **5i** and **5f** demonstrates their ligand-receptor affinity, better than that of the drug pentamidine, giving us the possibility of obtaining promising molecules in the scope of creation of new prototypes to pharmaceuticals. The compound **5i** confers the best molecule synthesized when compared to the enzyme CDK2, which showed high selectivity for the enzyme of the parasite and low for the human. In turn, compound **5f** comprises the two classes of enzymes, both rCPB2.8 and CRK3, when dealing with interaction energy in the CRK3 enzyme and better van der Waals interactions in the rCPB2.8 enzyme.

The results showed the possibility of favorable interactions between the proposed new molecules and the selected enzymes for biological studies, with that there is an expectation of a future scientific collaboration for the execution of pharmacological tests *in vivo* and *in vitro* for confirmation and correlation of observed results *in silico* and the search for progress in the study, promising in the area.

Supplementary Information

Supplementary data associated with this article are available free of charge at <http://jbcs.sbq.org.br> as a PDF file.

Acknowledgments

This work was supported by CAPES, CNPq, Fapemig, INCT-INOVAR, RQ-MG and Unifal-MG.

Author Contributions

Mariana G. R. Silva was responsible for project administration and writing; Marcia P. Veloso for supervision, project administration, conceptualization and writing; Thaynan A. B. Chagas for methodology; Mirian M. Cordeiro for methodology; Levy B. Alves for methodology and data curation; Paloma A. G. Monti for methodology and investigation; Ruth V. Souza for methodology and investigation.

References

1. <http://www.who.int/topics/leishmaniasis/en/>, accessed in March 2021.
2. Singh, N.; Kumar, M.; Singh, R. K.; *J. Trop. Med.* **2012**, *5*, 485.
3. http://www.who.int/gho/neglected_diseases/leishmaniasis/en/, accessed in March 2021.
4. Secretaria de Vigilância em Saúde, Ministério da Saúde (SVS/MS), São Paulo, Brazil, available at http://www.saude.sp.gov.br/resources/ccd/apresentacao/simposio-iv/3._francisco_edilson_ferreira_lima_jr._cenarios_da_lv_e_perspectivas.pdf, accessed in March 2021.
5. Pedrique, B.; Strub-Wourgaft, N.; Some, C.; Olliaro, P.; Trouiller, P.; Ford, N.; Pécoul, B.; Bradol, J.-H.; *Lancet Global Health* **2013**, *1*, 331.
6. https://apps.who.int/iris/bitstream/handle/10665/44412/WHO_TRS_949_eng.pdf;jsessionid=69FEE008C6B5EAAF FDE3571470948269?sequence=1, accessed in March 2021.
7. Micheletti, A. C.; Beatriz, A.; *Rev. Virtual Quim.* **2012**, *3*, 268.
8. Azizi, H.; Hassani, K.; Taslimi, Y.; Najafabadi, H. S.; Papadopoulou, B.; Rafati, S.; *Parasitology* **2009**, *136*, 723.
9. Gillmor, S. A.; Craik, C. S.; Fletterick, R.; *Protein Sci.* **1997**, *6*, 1603.
10. St. Hilaire, P. M.; Sanderson, S. J.; Mottram, J. C.; Alves, L. C.; *Chem. Biochem.* **2000**, *1*, 115.
11. Turk, V.; Stoka, V.; Vasiljeva, O.; Renko, M.; Sun, T.; Turk, B.; Turk, D.; *Biochim. Biophys. Acta* **2012**, *1*, 1824.
12. Mottram, J. C.; Coombs, G. H.; Alexander, J.; *Curr. Opin. Microbiol.* **2004**, *7*, 375.
13. Pereira, F. O.; Mendes, J. M.; Lima, E. O.; *Med. Mycol. J.* **2013**, *51*, 507.
14. Cleghorn, L. A. T.; Woodland, A.; Collie, I. T.; Torrie, L. S.; Norcross, N.; Luksch, T.; Mpamhanga, C.; Walker, R. G.; Mottram, J. C.; Brenk, R.; Frearson, J. A.; Gilbert, I. H.; Wyatt, P. G.; *ChemMedChem* **2011**, *6*, 2214.
15. Pereira, F. S. S.; Saraiva, L. A.; Silveira, N. J. F.; Veloso, M. P.; *Rev. Eletrônica Farm.* **2013**, *10*, 11.
16. Prajapati, V. K.; Pandey, R. K.; *Drug Des., Dev. Ther.* **2017**, *6*, 69.
17. Costa, P. R. R.; *Rev. Virtual Quim.* **2009**, *1*, 58.
18. Newman, D. J.; Cragg, G. M.; *J. Nat. Prod.* **2016**, *79*, 629.
19. Dikusar, E. A.; Zhukovskaya, N. A.; Moiseichuk, K. L.; Zaleskaya, E. G.; Kurman, P. V.; Vyglazov, O. G.; *Russ. J. Appl. Chem.* **2008**, *81*, 643.
20. Ayati, A.; Falahati, M.; Irannejad, H.; Emami, S.; *Daru, J. Pharm. Sci.* **2012**, *20*, 46.
21. Chakravarti, B.; Akhtar, T.; Rai, B.; Yadav, M.; Akhtar-Siddiqui, J.; Dhar, S. K.; Thakur, R.; Singh, A. K.; Kumar, H.; Khan, K.; Pal, S.; Rath, S. K.; Lal, J.; Konwar, R.; Trivedi, A. K.; Datta, D.; Mishra, D. P.; Godbole, M. M.; Sanyal, S.; Chattopadhyay, N.; Kumar, A.; *J. Med. Chem.* **2014**, *19*, 8010.
22. Xie, Y.; Huang, Z.; Yan, H.; Li, J.; Ye, L.; Che, L.; Tu, S.; *Chem. Biol. Drug Des.* **2014**, *6*, 743.
23. Emami, S.; Falahati, M.; Banifatemi, A.; Moshiri, K.; Shafiee, A.; *Arch. Pharm. Pharm. Med. Chem.* **2002**, 335, 318.
24. Mott, B. T.; Ferreira, R. S.; Simeonov, A.; Jadhav, A.; Ang, K. K.; Leister, W.; Shen, M.; Silveira, J. T.; Doyle, P. S.; Arkin, M. R.; McKerrow, J. H.; Inglese, J.; Austin, C. P.; Thomas, C. J.; Shoichet, B. K.; Maloney, D. J.; *J. Med. Chem.* **2010**, *53*, 52.
25. Pao, W.; Miller, V.; Zakowski, M.; Doherty, J.; Politi, K.; Sarkaria, I.; Singh, B.; Heelan, R.; Rusch, V.; Fulton, L.; Mardis, E.; Kupfer, D.; Wilson, R.; Kris, M.; Varmus, H.; *Proc. Natl. Acad. Sci. U. S. A.* **2004**, *101*, 13306.
26. Mirjafary, Z.; Abdolib, M.; Saeidanc, H.; Kakanejadifardb, A. S.; Farniad, M. F.; *RSC Adv.* **2016**, *6*, 17740.
27. Sali, A.; Blundell, T. L.; *J. Mol. Biol.* **1993**, *234*, 779.
28. Laskowski, R. A.; Macarthur, M. W.; Moss, D. S.; Thornton, J.; *J. Appl. Cryst.* **1993**, *26*, 283.
29. Eisenberg, D.; Lüthy, R.; Bowie, J. U.; *Methods Enzymol.* **1997**, *277*, 396.
30. Wiederstein, M.; Sippl, M. J.; *Nucleic Acids Res.* **2007**, *35*, 407.
31. <https://www.rcsb.org/>, accessed in June 2020.
32. Coelho, C. M.; dos Santos, T.; Freitas, P. G.; Nunes, J. B.; Marques, M. J.; Padovani, C. G. D.; Júdice, W. A. S.; Camps, I.; da Silveira, N. J. F.; Carvalho, D. T.; Veloso, M. P.; *J. Braz. Chem. Soc.* **2018**, *4*, 715.
33. Altschul, S. F.; Gish, W.; Miller, W.; Myers, E. W.; Lipman, D. J.; *J. Mol. Biol.* **1990**, *215*, 403.
34. Pieper, U.; Webb, B. M.; Dong, G. Q.; Schneidman-Duhovny, D.; Fan, H.; Kim, S. J.; Khuri, N.; Spill, Y. G.; Weinkam, P.; Hammel, M.; Tainer, J. A.; Nilges, M.; Sali, A.; *Nucleic Acids Res.* **2014**, *42*, 336.
35. Waterhouse, A.; Bertoni, M.; Bienert, S.; Studer, G.; Tauriello, G.; Gumienny, R.; Heer, F. T.; Beer, T. A. P.; Rempfer, C.; Bordoli, L.; Lepore, R.; Schwede, T.; *Nucleic Acids Res.* **2018**, *46*, 296.
36. Laskowski, R. A.; Rullmann, J. A. C.; MacArthur, M. W.; Kaptein, R.; Thornton, J. M.; *J. Biomol. NMR* **1996**, *8*, 477.
37. *Schrödinger Release 2017-1: Maestro version 11.1*; Schrödinger, LLC, New York, USA, 2017.

38. Schrödinger Release 2017-1: *LigPrep*; Schrödinger, LLC, New York, USA, 2017.
39. Schrödinger Release 2017-1: *Schrödinger Suite 2017-1 Protein Preparation Wizard, Epik*; Schrödinger, LLC, New York, USA, 2017; *Impact*; Schrödinger, LLC, New York, USA, 2017; *Prime*; Schrödinger, LLC, New York, USA, 2017.
40. Schrödinger Release 2017-1: *MacroModel*; Schrödinger, LLC, New York, USA, 2017.
41. Schrödinger Release 2017-1: *Induced Fit Docking protocol, Glide*; Schrödinger, LLC, New York, USA, 2017; *Prime*; Schrödinger, LLC, New York, USA, 2017.
42. Schrödinger Release 2017-1: *Prime*; Schrödinger, LLC, New York, USA, 2017.
43. Schrödinger Release 2017-1: *Glide*; Schrödinger, LLC, New York, USA, 2017.
44. *The PyMOL Molecular Graphics System*; Schrödinger, LLC, New York, USA, 2017.
45. Barreiro, E. J.; Lima, M. E. F.; *J. Pharm. Sci.* **1992**, *81*, 1219.
46. Ranu, B. C.; Jana, U. A.; *J. Org. Chem.* **1999**, *64*, 6380.
47. Gopalsamy, A.; Ellingboe, J. W.; Mckew, J. C.; Yang, H.; *Bioorg. Med. Chem. Lett.* **2006**, *16*, 2978.
48. Li, C. B.; Cui, Y.; Zhang, W. Q.; Li, J. L.; Zhang, S. M.; Choi, M. C. K.; Chan, A. S. C.; *Chin. Chem. Lett.* **2002**, *13*, 95.
49. Surwase, S. M.; Mane, Y. D.; Surwase, M. M.; Khade, B. C.; *J. Heterocycl. Chem.* **2019**, *57*, 724.
50. Pauli, F. P.; Barreiro, E. J.; Barbosa, M. L. C.; *Rev. Virtual Quim.* **2018**, *10*, 1280.
51. Lipinski, C. A.; *Drug Discovery Today: Technol.* **2004**, *1*, 337.
52. Vicik, R.; Busemann, M.; Gelhaus, C.; Stiefl, N.; Scheiber, J.; Schmitz, W.; Schulz, F.; Mladenovic, M.; Engels, B.; Leippe, M.; Baumann, K.; Schirmeister, T.; *ChemMedChem* **2006**, *1*, 1126.
53. Fey, P.; Chartomatsido, R.; Kiefer, W.; Mottram, J. C.; Kersten, C.; Schirmeister, T.; *Eur. J. Med. Chem.* **2018**, *156*, 587.
54. de Luca, L.; Ferro, S.; Buemi, M. R.; Monforte, A. M.; Gitto, R.; Schirmeister, T.; Maes, L.; Rescifina, A.; Micale, N.; *Chem. Biol. Drug Des.* **2018**, *92*, 1585.
55. Grant, K. M.; Dunion, M. H.; Yardley, V.; Skaltsounis, A. L.; Marko, D.; Eisenbrand, G.; Croft, S. L.; Meijer, L.; Mottram, J. C.; *Antimicrob. Agents Chemother.* **2004**, *48*, 3033.
56. Pavia, D. L.; Lampman, G. M.; Kriz, G. S.; Vyvyan, J. A.; *Introduction to Spectroscopy*, vol. 3, 4th ed.; Cengage Learning: Washington, USA, 2010.
57. Silva, R. C.; Veiga, F.; Vilela, F. C.; Pereira, A. V.; Cunha, T. T. S.; Tesch, R.; Viegas, C.; Dias, D. F.; Giusti-Paiva, A.; Veloso, M. P.; Fraga, C. A. M.; *Lett. Drug Des. Discovery* **2019**, *16*, 10.

Submitted: November 11, 2020

Published online: April 8, 2021

